

PHOTO GALVANIC CELL FOR CONVERSION OF SOLAR ENERGY INTO
ELECTRICITY: AZURE B–SODIUM LAURYL SULPHATE SYSTEM



Archana Sharma¹, Monika Jangid², Mukesh Kumar Jangid³, K. M.
Gangotri⁴

Article History: Received: 20/04/2023

Revised: 12/05/2023

Accepted: 16.05.2023

Abstract

The photochemistry of dye plays an important role in clarifying and understanding the electron transfer reactions in photogalvanic cells, photoconductors, semiconductor photo-catalysis, etc. The present study reports the photogalvanic effect using a suitable surfactant, reductant, and photosensitizer for solar energy conservation. To improve the solar power generation and storage capacity of the system, the surfactant NaLS was used and compared with the system without surfactant. Experiments have shown that the surfactant not only reduces the cost but also increases the storage capacity (56.0 min) and conversion efficiency (0.28%) of the photogalvanic cell with NaLS.

Keywords: Photogalvanic cell, photogalvanic effect, azure-B, sodium lauryl sulphate, conversion efficiency.

I. INTRODUCTION

The implementation of plasmonic metals into semiconductors is a successful method to improve the performance of photocatalysts and photoelectrochemical cells. There are three major mechanisms or methods are known to transfer plasmonic energy from a metal to a semiconductor, which includes light scattering or trapping, plasmon-induced resonance energy transfer and hot electron injection which is also known as direct electron transfer.¹

Photogalvanic processes are conveniently defined as the various types of physical and chemical processes essential to the conversion of a flux of electromagnetic radiations into electrical power by means of a photogalvanic-device.² First of all in 1925 Rideal and Williams observed the photogalvanic effect³ but it was systematically investigated by Robinowitch in Fe[III] thionine system long back.^{4,5} Becquerel first observed the flow of current between two unsymmetrical illuminated metal electrodes in sunlight.⁶

A photogalvanic device is taken to be a battery in which the cell solution absorbs light directly to generate species, which upon back reaction through an external circuit with the aid of suitable electrode produces electric power. The charge carrying species have storage capacity if they are long lived.⁷⁻⁹ The Photogalvanic cells uses very dilute solutions of sensitizer(s), surfactants and reductants in basic or acidic medium for solar power generation and storage.¹⁰⁻¹⁵ The power from the cell is extracted by dipping two electrodes a working and a counter electrodes in the solution.¹⁶⁻¹⁸

The photochemistry of dye plays an important role to clarify and understand the electron transfer reactions in photogalvanic cells, photoconductors, semiconductor photo-catalysis, etc. Oxazines and thiazines dyes have been used widely as a photosensitizer with and without surfactants in the photogalvanic cells for solar power conversion and storage.¹⁹⁻²² Since, the stability and solubility of photosensitizers (dyes) are increased in the presence of surfactant and these properties lead to enhance the electrical output of the photogalvanic cells.²³⁻²⁴

Pan et al.²⁵ developed thiazine based photoelectrochemical cell; which involves photo-reduction of thiazine using EDTA, which act as the electron donor and photosynthetic electron transporter to chloroplasts for the generation of electricity. They conclude by the observations that energy conversion efficiency may be increased by combining the thiazine photogalvanic cell with the chloroplast solar battery.

Gangotri, and Regar²⁶ studied the photogalvanic effect cells which contain safranin as photosensitizer, and glucose, EDTA, and NTA as reductants in different systems. They observed that in case of EDTA–safranin system, the photopotential and photocurrent generated were 760 mV and 50 μ A, while in case of glucose–safranin system it is 373 mV and 35 μ A and in case of NTA–safranin system

it is 415 mV and 35 μ A in, respectively. They also studied the effects of different parameters on electrical output of the cells.

Mall et al.²⁷ studied the level of interaction of different dyes with sodium dodecyl sulphate (SDS), to find out the dye–SDS order. They observed that Brilliant Cresyl Blue, Azur A Nile Blue O, and TB O shows red shift while methylene blue, Azure B, and Azure C shows blue shift in their λ_{max} , which indicates the formation of dye–surfactant complex. They observed that dyes with red shifting have greater stability in excited state as well as higher electrical output data of the cell than dye with blue shifting. They conclude that the dye–surfactant complex have greater stability in excited state which will be more useful for improvement of conversion efficiency and storage capacity of photogalvanic cells.

Suriani et al.²⁸ used 4-bis(neopentyloxy)-3-(neopentyloxycarbonyl)-1,4-dioxobutane-2-silphonate surfactant assisted reduced graphene oxide (rGO) in dye-sensitized solar cell as a counter electrode. They observed that TC14-rGO modified CE based solar cell shows 0.828% power conversion efficiency and 2.72 mA cm⁻² short current density and 0.65 V open circuit voltage which were higher as compared to counter electrode fabricated from commercially available SDS surfactant assisted rGO. They conclude that TC14-rGO act as a potential counter electrode material to construct efficient dye-sensitized solar cell.

Genwa, and Kumar²⁹ used methyl green to study the performance of dye-sensitized photogalvanic cells for the conversion of solar energy to electrical energy. They prepare a system using methyl green as the photosensitizer (dye) and DTPA as the reducing agent in the presence of sodium lauryl sulphate. They studied the effect of various rate affecting parameters such as effect of the dye, concentration of surfactant and reductant, light intensity, temperature, and electrode area, on electrical output of the cell. They observed that photopotential and photocurrent generated by this system were 815 mV and 310 μ A, respectively.

In current scenario, where there is a need of solar energy to fulfill the need of energy, the present study of preparation of galvanic cell using azure B and Sodium lauryl system is evaluated for the conversion of solar energy into the electrical energy.

II. MATERIAL, METHOD AND MECHANISM

The following chemicals are used in the present work: Azur-B (LOBA), Dodecyl Sulphate Sodium salt (HIMEDIA) (Sodium lauryl sulphate), D(+) Mannose (LOBA), Sodium hydroxide, Oxalic Acid, Phenolphthalein. In the experiment Azur-B as photosensitizer (M/500), Mannose (M/100), surfactants NaLS (M/100), Tween-80 (M/100) and CPC (M/100) and NaOH (1M) were prepared in double distilled water and kept in Amber coloured container to protect from sun light. A H-shaped glass tube is used which consist of known amount of the solutions of photosensitizer (dye), Sodium hydroxide, Reductant, surfactant and distilled water so as to keep the total volume of the mixture always 25.0 ml. A platinum electrode (1.0 \times 1.0 cm²) is dipped in one limb and a Saturated Calomel Electrode (SCE) is immersed in the another limb of the H-tube. The terminals of the electrode are then connected to a digital pH meter (Systronics Model – 335) and the whole cell is placed in the dark. The potential (mV) is measured in dark when the cell attains a stable potential. Then the limb containing platinum electrode is exposed to a 200 W tungsten lamp (Philips). The Light intensity is varied by employing lamps of different wattage. A water filter is placed between the illuminated chamber and the light source to cut-off infra-red radiations.

III. MECHANISM

The reactions between surfactant and dye do not effectively react at dark. It may be concluded that the redox potential of reductant Mannose is much higher than that of the used dye. It was observed that a rapid fall in potential reaches a static value after some period. On removing the source of illumination, the directions of change of potential were reversed; however, it never reached the initial value. It suggests that the main reversible photochemical reaction is also accompanied by some irreversible side reactions.

Clark and Eckert³⁰ have reported about the electroactive species in well established photogalvanic systems like iron (II) thionine where ferric ions were considered as reactive species at the dark electrode, but in all the three surfactants Mannose – AB photogalvanic systems the electroactive species are quite different. The Leuco dye and the dye itself are the electroactive species at the illuminated and dark electrode, respectively.

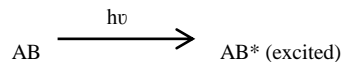
On illumination the photocurrent was increased rapidly in first few minutes to reaching a maximum (i_{max}), the increase in diffusion length did not affect the photocurrent at equilibrium (i_{eq}) and

also the (i_{eq}), should be recycling reaction of the oxidation product of reducing agent and the semi or leuco dye.

The participation of leuco-forms of the dye as electroactive species was experimentally confirmed by Wildes and Lichtin³¹ and Wyarnt Remyetal.³² It is to be mentioned that photo-decay and deactivation of dye follows non-zero order kinetics. On the basis of observations, the mechanism for photogeneration of electricity has also been proposed as

Illuminated Chamber

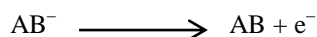
On irradiation, dye molecules get excited



The excited dye molecules accept an electron from reductant and converted into semi or leuco form of dye, and the reductant into its excited form



At Pt electrode, the semi or leuco form of dye loses an electron and converted into original dye molecule

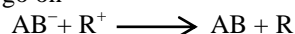


Dark Chamber

At counter electrode, dye molecule accept an electron from electrode and converted in semi or leuco form



Finally, leuco/semi form of dye and oxidized form of reductant combine to give original dye and reductant. Molecule and the cycle will go on



Where,

AB = dye, AB* = excited form of dye, AB⁻ = semi or leuco form of dye, R = reducing form of the reductant and R⁺ = oxidized form of the reductant.

IV. RESULT AND DISCUSSION

A. Variation of Potential with Time

The photogalvanic cell is placed in dark till it attained a stable potential and then the platinum electrode is exposed to light. It is observed that potential changes on illumination and it reaches a constant value after a certain period. When the light source is removed, the direction of change in potential are reversed and a stable potential are again obtained after sometime. The effect of variation of potential with time on NaLS-Mannose- Azur-B system studied in the range of ~ 2 hrs and the results are reported in Table 1 and Fig. 1 A and 1B.

Table 1: Variation of Potential with Time

NaLS-Mannose-Azur-B system		Mannose- Azur-B system [without surfactant]	
[NaLS] = 6.00×10^{-4} [Mannose] = 1.68×10^{-3} [Azur-B] = 5.28×10^{-5}		Light Intensity = 10.4 mW cm^{-2} Temp. = 303K pH = 12.48	
		[Mannose] = 1.60×10^{-3} [Azur-B] = 5.20×10^{-5} pH = 12.17	
Time (Min)	Potential (mV)	Time (Min)	Potential (mV)
0.0	-163.0	0.0	-174.0
5.0	-179.0	58.0	-185.0
10.0	-183.0	10.0	-187.0
15.0	-194.0	15.0	-204.0
20.0	-203.0	20.0	-226.0
25.0	-212.0	25.0	-290.0
30.0	-288.0	30.0	-384.0
35.0	-354.0	35.0	-470.0
40.0	-370.0	40.0	-521.0
45.0	-410.0	45.0	-562.0
50.0	-440.0	50.0	-584.0
55.0	-499.0	55.0	-587.0
60.0	-588.0	60.0	-599.0
65.0	-659.0	65.0	-605.0
70.0	-848.0	70.0	-612.0
75.0	-1125.0	75.0	-633.0
80.0	-1125.0	80.0	-1005.0
85.0	-1125.0	85.0	-1005.0
90.0	-1125.0 (light off)	90.0	-1005.0
95.0	1123.0	95.0	-1005.0
100.0	1120.0	100.0	-1005.0 (lights off)
105.0	1113.0	105.0	-998.0
110.0	1109.0	110.0	-998.0

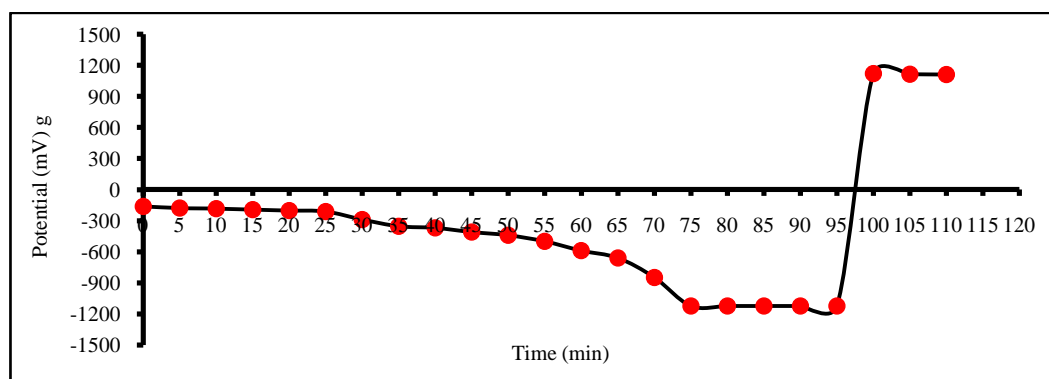


Fig. 1A: Variation of potential with time (NaLS-Mannose-Azure B System with surfactant)

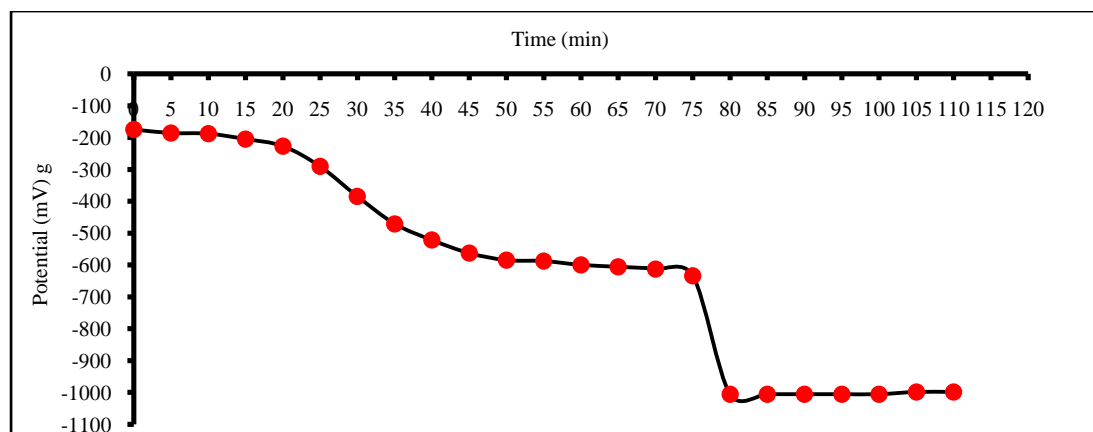


Fig. 1 B: Variation of potential with time (NaLS-Mannose-Azure B System [without surfactant])

B. Variation of Current with Time

It is observed that a rapid rise in photocurrent of NaLS–Mannose–Azur B system on illumination and it reaches a maximum within few minutes. This value is denoted by i_{max} . Then the current are found to decrease gradually with the period of illumination finally reaching a constant value at equilibrium. This value is represented as i_{eq} . Same trend is followed in the Mannose–Azur B system (without surfactant).The current is found to decrease on removing the source of illumination. The variation of current in this system i.e. NaLS–Mannose–Azur B with respect to time and in the Mannose–Azur B system (without surfactant) is given in Table 2.

Table 2: Variation of Current with Time

NaLS-Mannose-Azur B system		Mannose- Azur B system [without surfactant]	
[NaLS] = 6.00×10^{-4} Light Intensity = 10.4 mW cm^{-2} [Mannose] = 1.68×10^{-3} Temp. = 303K [Azur-B] = 5.28×10^{-5} pH = 12.48		[Mannose] = 1.60×10^{-3} [Azur-B] = 5.20×10^{-5} pH = 12.17	
Time (Min)	Current (μA)	Time (Min)	Current (μA)
0.0	0.0	0.0	0.0
2.0	85.0	1.0	18.0
3.0	96.0	2.0	29.0
4.0	110.0	3.0	35.0
5.0	122.0	4.0	45.0
6.0	130.0	5.0	52.0
10.0	126.0	5.5	55.0
20.0	119.0	6.0	67.0
30.0	114.0	6.5	75.0
40.0	110.0	7.0	73.0
50.0	104.0	10.0	70.0
60.0	99.0	20.0	66.0
65.0	95.0	30.0	62.0
70.0	89.0	40.0	57.0
75.0	85.0	50.0	53.0
80.0	85.0	60.0	49.0
85.0	85.0	70.0	44.0
90.0	85.0 (light off)	80.0	40.0
100.0	80.0	90.0	40.0
110.0	77.0	100.0	40.0 (lights off)
115.0	74.0	110.0	38.0
120.0	73.0	120.0	35.0
125.0	70.0	125.0	35.0

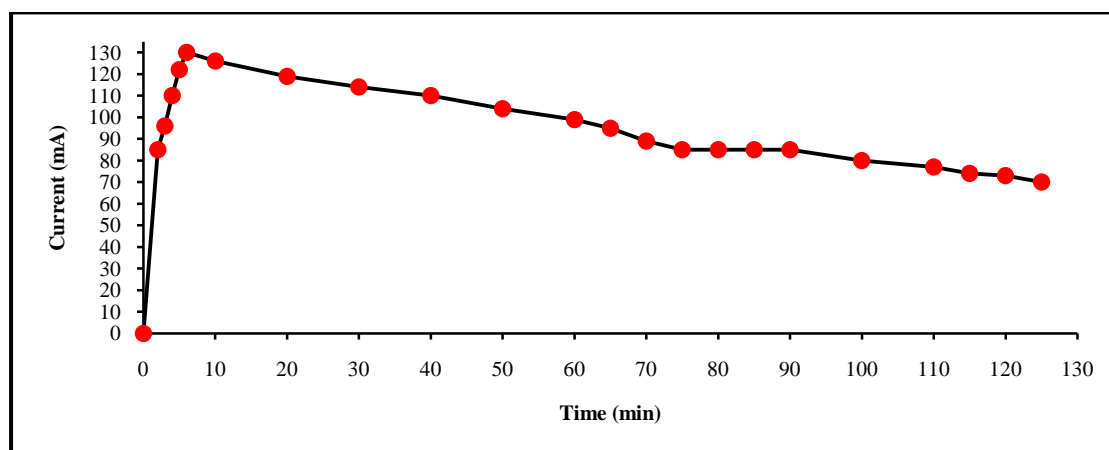


Fig. 3.2 (A): Variation of current with time (NaLS-Mannose-Azure B System with surfactant)

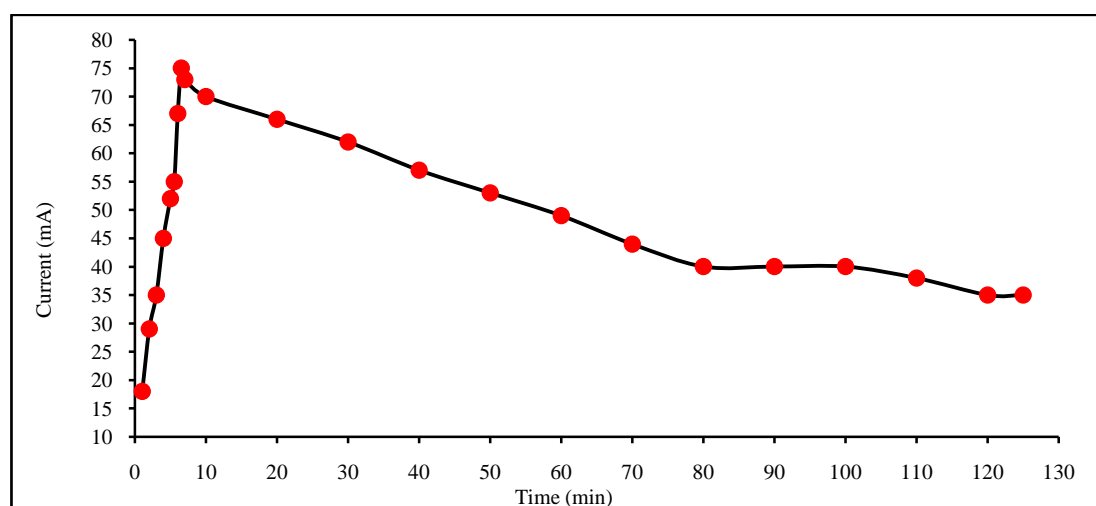


Fig. 3.2 (B): Variation of current with time (Mannose-Azure B System without surfactant)

C. Effect of variation of pH

Photogalvanic cell containing NaLS–Mannose–Azur-B system are found to be quite sensitive to the pH of the solution. It is observed that there is an increase in the photopotential of this system with the increase in pH value (In the alkaline range). At pH = 12.48 a maxima is obtained for NaLS-Mannose-Azur-B system whereas in the Mannose-Azur-B system at pH 12.17 a maxima is obtained. On further increase in pH, there is a decrease in photopotential. Consequently the conversion efficiency also shows the same trend but the storage capacity of the photogalvanic cell was observed in irregular manner. The effect of variation of pH concentration on conversion efficiency and storage capacity of NaLS-Mannose-Azur-B system and Mannose-Azure-B system (without surfactant) are reported in Table 3.

Table 3: Effect of variation of pH

NaLS-Mannose-Azur-B system	Mannose- Azur-B system [without surfactant]
$[\text{NaLS}] = 6.00 \times 10^{-4}$ $[\text{Mannose}] = 1.68 \times 10^{-3}$ $[\text{Azur-B}] = 5.28 \times 10^{-5}$	$[\text{Mannose}] = 1.60 \times 10^{-3}$ $[\text{Azur-B}] = 5.20 \times 10^{-5}$
Light Intensity = 10.4 mW cm^{-2} Temp. = 303K	

NaLS- Mannose-Azur-B system	pH				
	12.00	12.20	12.48	12.63	12.81
Conversion efficiency	0.1530	0.2160	0.2795	0.2360	0.1954
Storage capacity (min.) (in dark)	42.0	51.0	56.0	50.0	44.0
Mannose-Azur-B system (Without surfactant)					
Conversion efficiency	0.599	0.904	0.1028	0.873	0.624
Storage capacity (min.) (in dark)	11.0	18.0	21.0	15.0	19.0

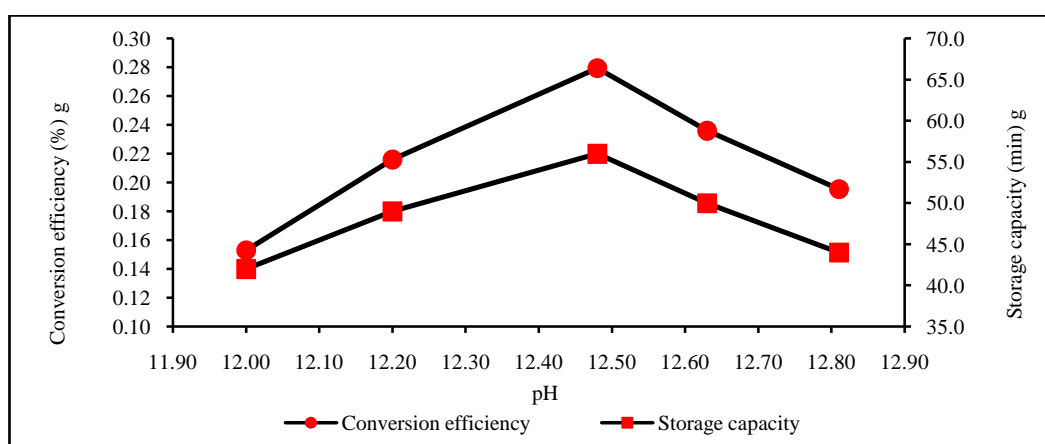


Fig. 3.3: Variation of conversion efficiency and storage capacity with pH

D. Effect of Variation of [NaLS] Concentration

Electrical output of the cell is found to increase on increasing the concentration of NaLS reaching a maximum value. On further increase in their concentration, a fall in photopotential, photocurrent and power of photogalvanic cell is obtained. Consequently the conversion efficiency also shows the same trend but the storage capacity of the photogalvanic cell was observed in irregular manner. The effect of variation of NaLS concentration on conversion efficiency and storage capacity of NaLS-Mannose-Azur-B system is reported in Table 4.

Table 4: Effect of variation of [NaLS] Concentration

[Mannose] = 1.68×10^{-3} Light Intensity = 10.4 mW cm^{-2} [Azur-B] = 5.28×10^{-5} Temp. = 303K pH = 12.48		[NaLS] $\times 10^{-4}$ M				
NaLS- Mannose-Azur-B system		5.00	5.50	6.00	6.50	7.00
Conversion efficiency		0.1781	0.2178	0.2795	0.2345	0.1831
Storage capacity (min.) (in dark)		47.0	50.0	56.0	53.0	49.0

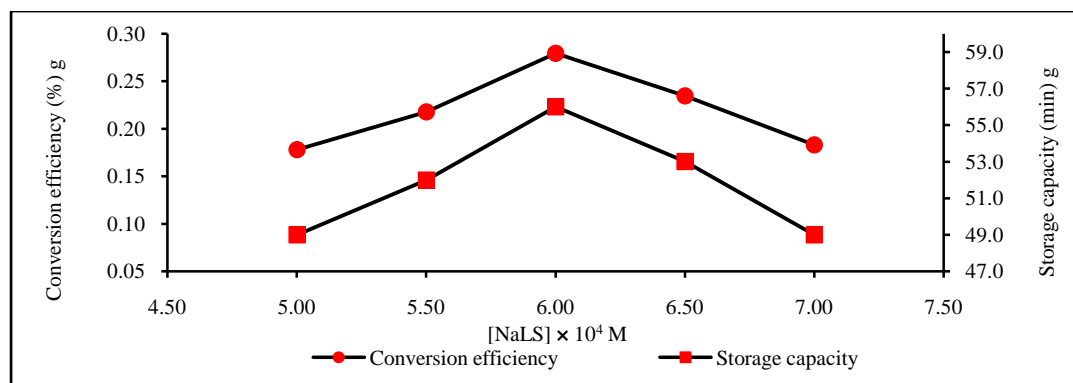


Fig. 3.4: Variation of conversion efficiency and storage capacity with [NaLS] concentration

E. Effect of Variation of [Mannose] Concentration

With the increase in concentration of the reductant [Mannose] the photopotential is found to be increase till it reaches a maximum. On further increase in concentration of Mannose a decrease in the electrical output of the cell is observed.

Consequently the conversion efficiency also shows the same trend but the storage capacity of the photogalvanic cell was observed in irregular manner. The effect of variation of Mannose concentration on conversion efficiency and storage capacity of NaLS-Mannose-Azur-B system and Mannose-Azur-B system (without surfactant) are reported in Table 5.

Table 5: Effect of variation of [Mannose] concentration

NaLS-Mannose-Azur-B system	Mannose- Azur-B system [without surfactant]				
[NaLS] = 6.00×10^{-4} [Azur-B] = 5.28×10^{-5} pH = 12.48	Light Intensity = 10.4 mW cm^{-2} Temp. = 303K				
	[Azur-B] = 5.20×10^{-5} pH = 12.17				
NaLS– Mannose–Azur-B system	[Mannose] × 10 ⁻³ M				
	1.20	1.42	1.68	1.82	2.00
Conversion efficiency	0.2067	0.2120	0.2795	0.2045	0.1870
Storage capacity (min.) (in dark)	34.0	44.0	56.0	43.0	30.0
Mannose-Azur-B system (Without surfactant)	1.23	1.49	1.60	1.89	2.12
Conversion efficiency	0.793	0.999	0.1028	0.973	0.886
Storage capacity (Min.) (in dark)	13.0	16.0	21.0	18.0	11.0

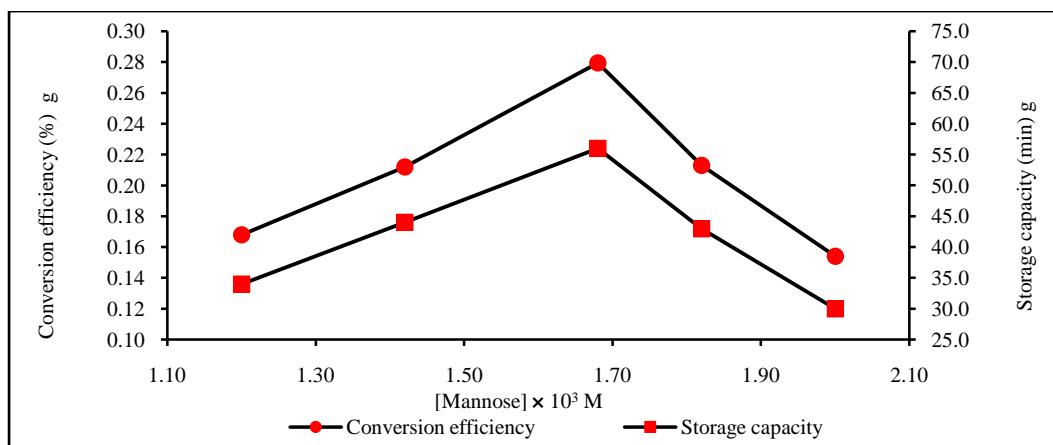


Fig. 3.4 (A): Effect of variation of conversion efficiency and storage capacity with [Mannose] concentration

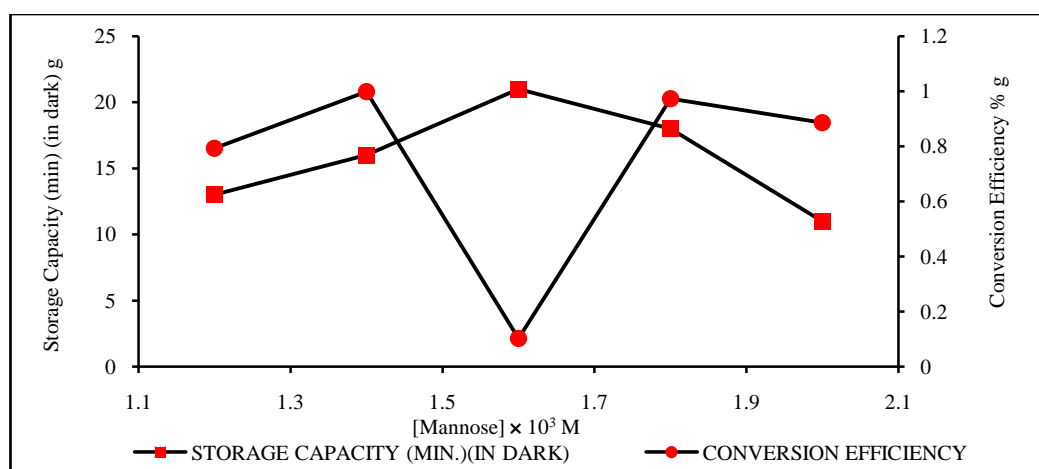


Fig. 3.4 (B): Effect of variation of conversion efficiency and storage capacity with [Mannose] concentration without surfactant

F. Effect of Variation of [Azur-B] Concentration

It is observed that the conversion efficiency and storage capacity are increased with the increase in concentration of the dye. A maxima is obtained for a particular value of Azur-B concentration, above which a decrease in the electrical output of the cell is obtained. Consequently the conversion efficiency also shows the same trend but the storage capacity of the photogalvanic cell was observed in irregular manner. The effect of variation of Azur-B concentration on conversion efficiency and storage capacity of NaLS-Mannose-Azur-B system and Mannose-Azur-B system (without surfactant) are reported in Table 6.

Table 6: Effect of variation of [AB] Concentration

NaLS-Mannose-Azur-B system	Mannose- Azur-B system [without surfactant]				
[NaLS] = 6.00×10^{-4} [Mannose] = 1.68×10^{-3} pH = 12.48	Light Intensity = 10.4 mW cm^{-2} Temp. = 303K				
	[Mannose] = 1.60×10^{-3} pH = 12.17				
	[Azur-B] × 10 ⁻⁵ M				
NaLS- Mannose-Azur-B system	4.80	5.09	5.24	5.48	5.60
Conversion efficiency	0.1123	0.2402	0.2795	0.2073	0.1316

Storage capacity (min.) (in dark)	30.0	44.0	56.0	45.0	29.0
Mannose-Azur-B system (Without surfactant)	4.80	5.01	5.20	5.42	5.68
Conversion efficiency	0.598	0.701	0.1028	0.787	0.623
Storage capacity (in dark)	11.0	17.0	21.0	19.0	13.0

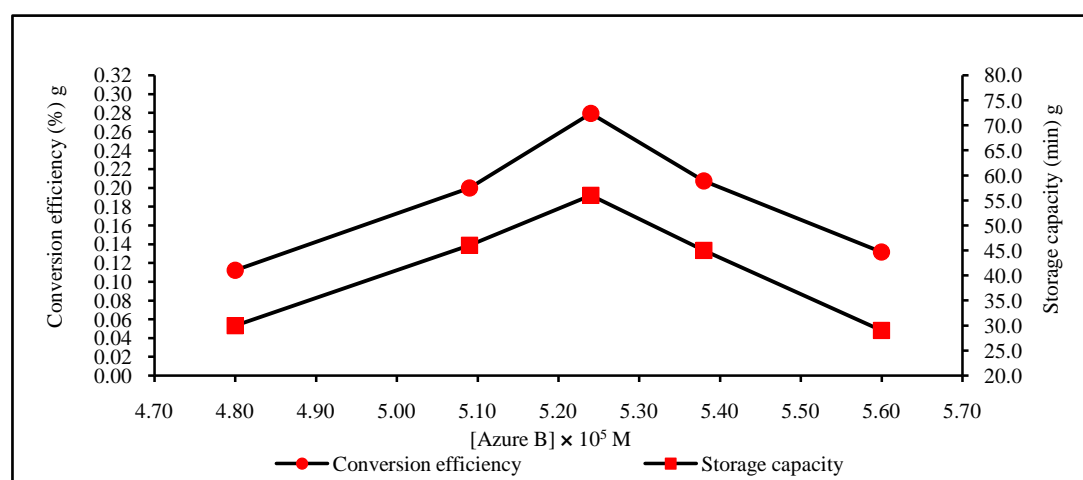


Fig. 3.4 (A): Variation of Conversion efficiency and Storage capacity with [Azure B] Concentration

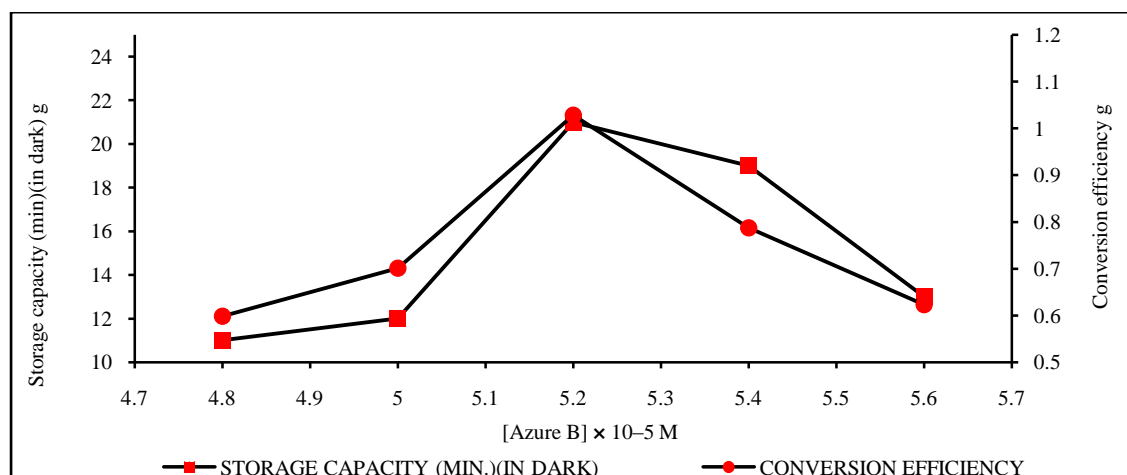


Fig. 3.6 (B): Effect of variation of azure B concentration (Mannose- AB system [without surfactant])

G. *i*-*V* Characteristics of the Cell

The short circuit current (i_{sc}) and open circuit voltage (V_{oc}) of the photogalvanic cells are measured with the help of a multimeter (keeping the circuit closed) and with a digital pH meter (keeping the other circuit open), respectively. The current and potential values in between these two extreme values are recorded with the help of a carbon pot (log 470 K) connected in the circuit of multimeter, through which an external load is applied. The *i*-*V* characteristics of the photogalvanic cells containing NaLS-Mannose-Azur-B system and Mannose-Azur-B system (without- surfactant) are given in Table 7.

Table 7: Current-Voltage (*i*-*V*) characteristics of the cell

NaLS-Mannose-Azur-B system	Mannose- Azur-B system [without surfactant]
----------------------------	--

[NaLS] = 6.00×10^{-4}		Light Intensity = 10.4 mW cm^{-2}		[Mannose] = 1.60×10^{-3}	
[Mannose] = 1.68×10^{-3}		Temp. = 303 K		[Azur-B] = 5.20×10^{-5}	
[Azur-B] = 5.28×10^{-5}		pH = 12.48		pH = 12.17	
Potential (mV)*	Photocurrent (μA)	Fill Factor (η)	Potential (mV)*	Photocurrent (μA)	Fill Factor (η)
-1125.0	0.0		-1005.0	0.0	
-1099.0	5.0		-960.0	5.0	
-1001.0	10.0		-815.0	10.0	
-956.0	15.0		-712.0	15.0	
-873.0	20.0		-678.0	20.0	0.2680
-780.0	25.0		-490.0	25.0	
-691.0	30.0		-372.0	30.0	
-678.0	35.0		-289.0	35.0	
-545.0	40.0		0.0	40.0	
-499.0	45.0	0.3083			
-444.0	50.0				
-398.0	55.0				
-324.0	60.0				
-278.0	65.0				
-204.0	70.0				
-189.0	75.0				
-137.0	80.0				
0.0	85.0				

* Absolute value

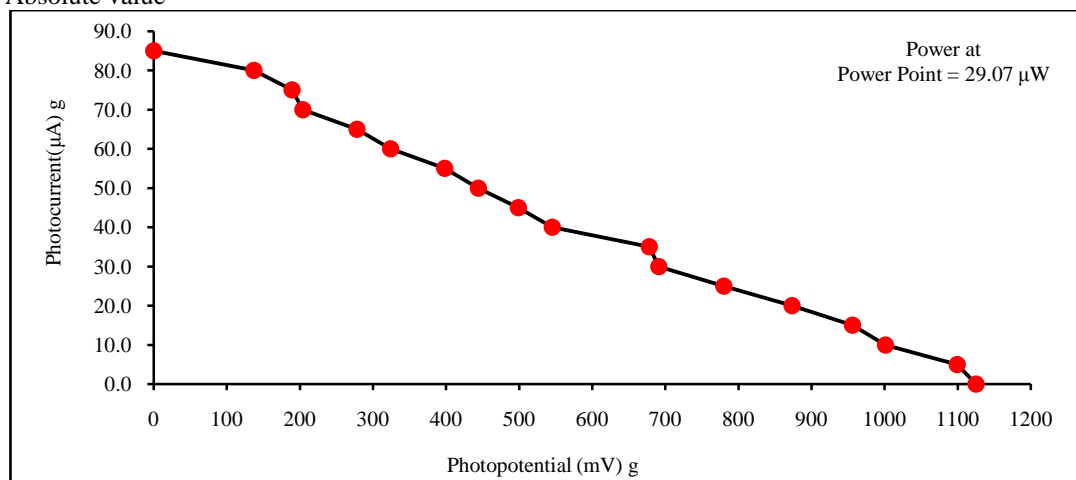


Fig. 3.5 (A): Current–voltage (i-V) characteristics of the cell

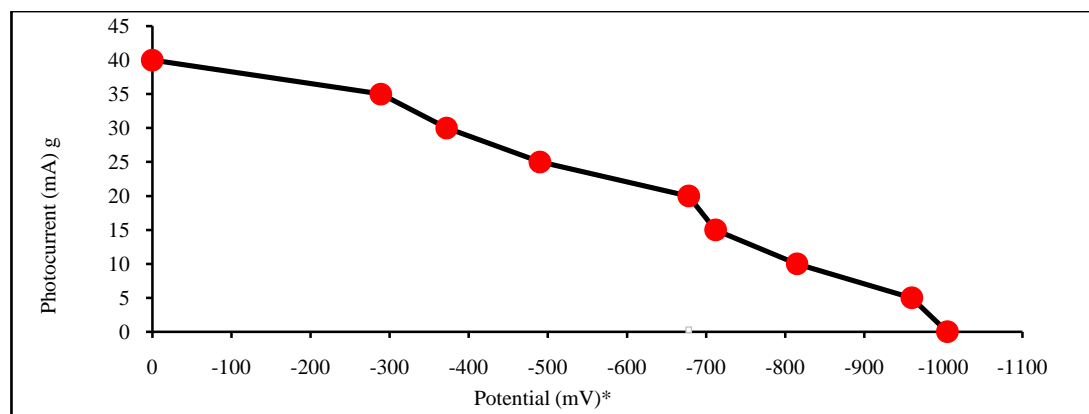


Fig. 3.5 (A): Current–voltage (i-V) characteristics of the cell (Mannose–Azure B system [without surfactant])

It is observed that i-V curve deviated from their regular rectangular shapes. A point in i-V curve, called Power Point (pp) is determined where the product of current and potential is maximum and the fill-factor is calculated using the formula:

$$\text{Fill factor } (\eta) = \frac{V_{pp} \times i_{pp}}{V_{oc} \times i_{sc}}$$

Where, V_{pp} and i_{pp} = the value of potential and current at power point, V_{oc} and i_{sc} = open circuit voltage and short circuit current, respectively.

H. Effect of Diffusion Length

The effect of variation of Diffusion Length (distance between the two electrodes) on the current parameters of the cell (i_{max} , i_{eq}) and initial rate of generation of photocurrent) are studied using H-shaped cell of different dimensions. It is observed that with an increase in diffusion length (i_{max}), and rate ($\mu\text{A min}^{-1}$) both showed an increase but the (i_{eq}) showed a negligibly small decreasing behaviour with the increase in diffusion length. So, virtually, it may be considered as unaffected by the changes in diffusion length. The results are summarized for NaLS-Mannose-Azur-B system and for Mannose-Azur-B system (without surfactant) in Table 8.

Table 8: Effect of diffusion length

NaLS-Mannose-Azur-B system		Mannose- Azur-B system [without surfactant]	
[NaLS] = 6.00×10^{-4} [Mannose] = 1.68×10^{-3} [Azur-B] = 5.28×10^{-5}		Light Intensity = 10.4 mW cm^{-2} Temp. = 303K pH = 12.48	
		[Mannose] = 1.60×10^{-3} [Azur-B] = 5.20×10^{-5} pH = 12.17	
Diffusion Length D_L (mm)	Maximum photocurrent $i_{max}(\mu\text{A})$	Equilibrium photocurrent $i_{eq}(\mu\text{A})$	Rate of initial generation of current ($\mu\text{A min}^{-1}$)
NaLS-Mannose-AB system			
35.0	127.0	95.0	18.8
40.0	129.0	90.0	27.2
45.0	130.0	85.0	21.6
50.0	132.0	82.0	22.0
55.0	133.0	80.0	22.4
Mannose-AB system (Without Surfactant)			
35.0	65.0	50.0	10.5

40.0	70.0	45.0	11.0
45.0	75.0	40.0	11.5
50.0	80.0	36.0	12.0
55.0	85.0	30.0	12.5

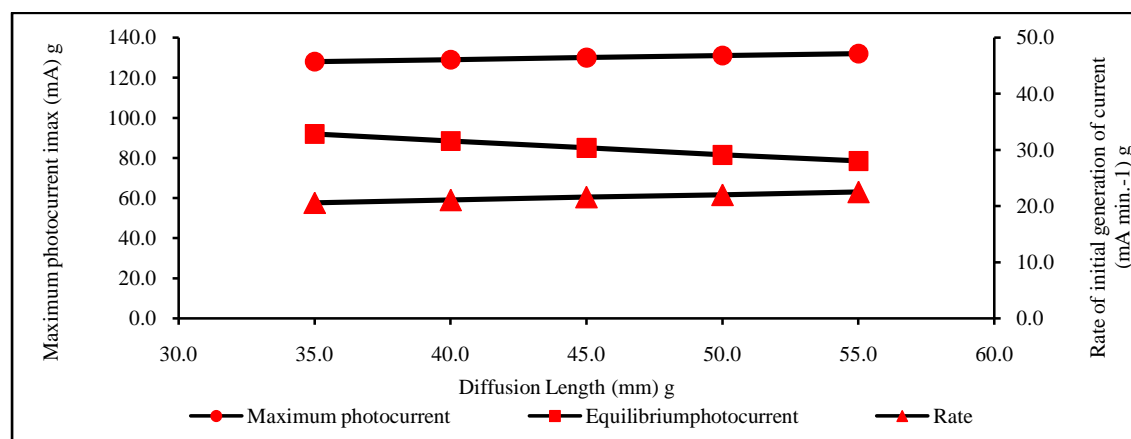


Fig. 3.6 (A): Variation of Current Parameters with Diffusion Length

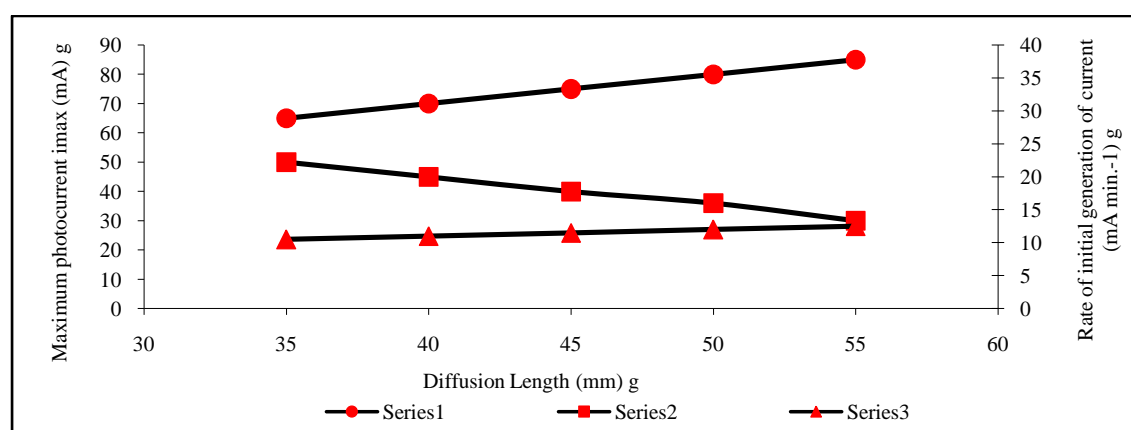


Fig. 3.6 (B): Variation of current parameters with diffusion length (Mannose–Azure B system [without surfactant])

1. Effect of Electrode Area

The effect of electrode area on the current parameters of the cell is also studied. It is observed that with the increase in the electrode area, the value of maximum potential (i_{max}) is found almost independent of this variation (rather it is affected in reverse manner). The effect of variation of electrode area on i_{max} and i_{eq} is reported in following table for the NaLS-Mannose-Azur-B system and for the Mannose-Azur-B system (without surfactant).

Table 9: Effect of electrode area

NaLS-Mannose-Azur-B system	Mannose- Azur-B system [without surfactant]				
[NaLS] = 6.00×10^{-4} [Mannose] = 1.68×10^{-3} [Azur-B] = 5.28×10^{-5}	Light Intensity = 10.4 mW cm^{-2} Temp. = 303K pH = 12.48				
	[Mannose] = 1.60×10^{-3} [Azur-B] = 5.20×10^{-5} pH = 12.17				
NaLS– Mannose–Azur-B system	Electrode Area (cm ²)				
	0.36	0.64	1.00	1.44	1.69

Maximum photocurrent (i_{\max}) (μA)	111.0	116.0	130.0	142.0	156.0
Equilibrium photocurrent (i_{eq}) (μA)	99.0	91.0	85.0	80.0	76.0
Mannose–Azur-B system (without surfactant)					
Maximum photocurrent i_{\max} (μA)	56.0	69.0	75.0	89.0	108.0
Equilibrium photocurrent i_{eq} (μA)	50.0	46.0	40.0	34.0	28.0

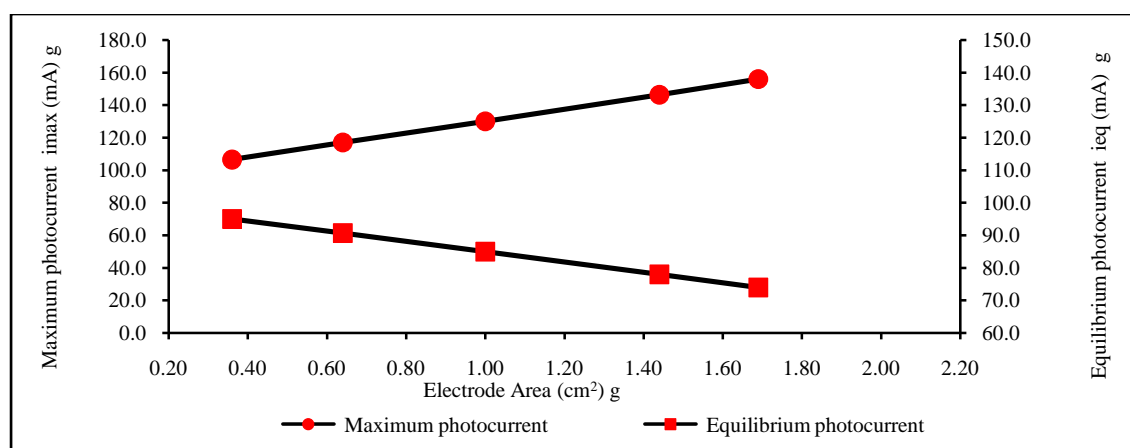


Fig. 3.7: Variation of current parameters with electrode area

J. Effect of Temperature

With an increase in the temperature, the photocurrent of the photogalvanic cell is found to increase with a corresponding rapid fall in potential. Consequently the conversion efficiency also shows the same trend but the storage capacity of the photogalvanic cell was observed in irregular manner. The results are reported in Table 10 for NaLS-Mannose-Azur-B system and for Mannose-Azur-B system (without surfactant).

Table 10: Effect of temperature

NaLS-Mannose-Azur-B system		Mannose- Azur-B system [without surfactant]				
[NaLS] = 6.00×10^{-4} Light Intensity = 10.4 mW cm^{-2}		[Mannose] = 1.60×10^{-3}				
[Mannose] = 1.68×10^{-3} pH = 12.48		[Azur-B] = 5.20×10^{-5}				
[Azur-B] = 5.28×10^{-5}		pH = 12.17				
NaLS– Mannose –Azur-B system	Temperature (K)					
	298.0	303.0	309.0	315.0	320.0	
Conversion efficiency	0.2936	0.2795	0.2018	0.1901	0.1823	
Storage Capacity (min.) (In dark)	50.0	56.0	59.0	62.0	64.0	
Mannose–Azur-B system (without surfactant)						
Conversion efficiency	0.1382	0.1028	0.849	0.683	0.565	
Storage Capacity (min.) (In dark)	15.0	21.0	29.0	36.0	48.0	

The effect of temperature on total possible power output in the NaLS-Mannose-Azur-B system and Mannose-Azur-B system (without surfactant) are also studied and it is observed that with the increase in temperature (temperature range under observation) the power output of the cell increase slowly irrespective of the rapid fall in photopotential.

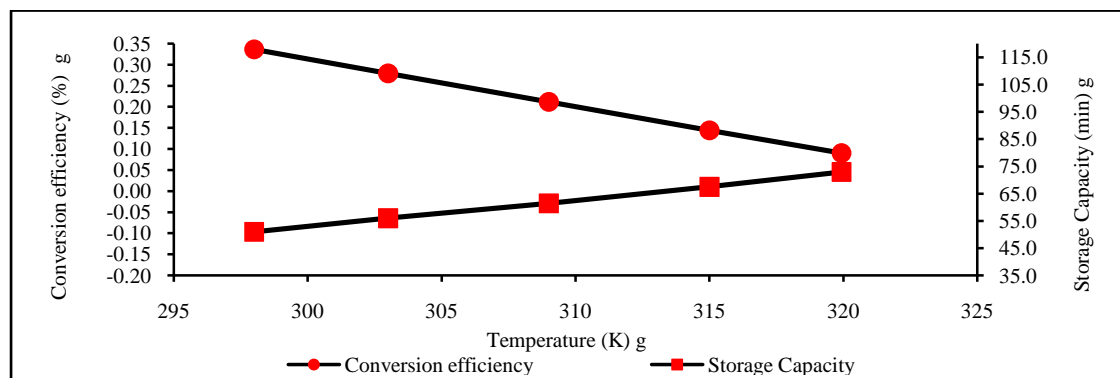


Fig. 3.8: Variation of conversion efficiency and storage capacity with temperature

K.Effect of Light Intensity

It is found that photocurrent showed a linear increasing behaviour with the increase in light intensity whereas photopotential increases in a logarithmic manner. Consequently the conversion efficiency also shows the same trend but the storage capacity of the photogalvanic cell was observed in irregular manner. The result are reported in given table for NaLS-Mannose-Azur-B system and for Mannose-Azur-B system (without surfactant).

Table 11: Effect of light intensity

NaLS-Mannose-Azur-B system		Mannose- Azur-B system [without surfactant]	
[NaLS] = 6.00×10^{-4} Temp. = 303K		[Mannose] = 1.60×10^{-3}	
[Mannose] = 1.68×10^{-3} pH = 12.48		[Azur-B] = 5.20×10^{-5}	
[Azur-B] = 5.28×10^{-5}		pH = 12.17	
NaLS– Mannose –Azur-B system	Light intensity (mW cm^{-2})		

	3.2	5.0	10.4	15.0	25.0
Conversion efficiency	0.2290	0.2463	0.2795	0.2811	0.2982
Storage Capacity (min.) (In dark)	49.0	53.0	56.0	58.0	62.0
Mannose –Azur-Bsystem (without surfactant)					
Conversion efficiency	0.842	0.963	0.1028	0.1121	0.1341
Storage Capacity (min.) (In dark)	14.0	18.0	21.0	23.0	26.0

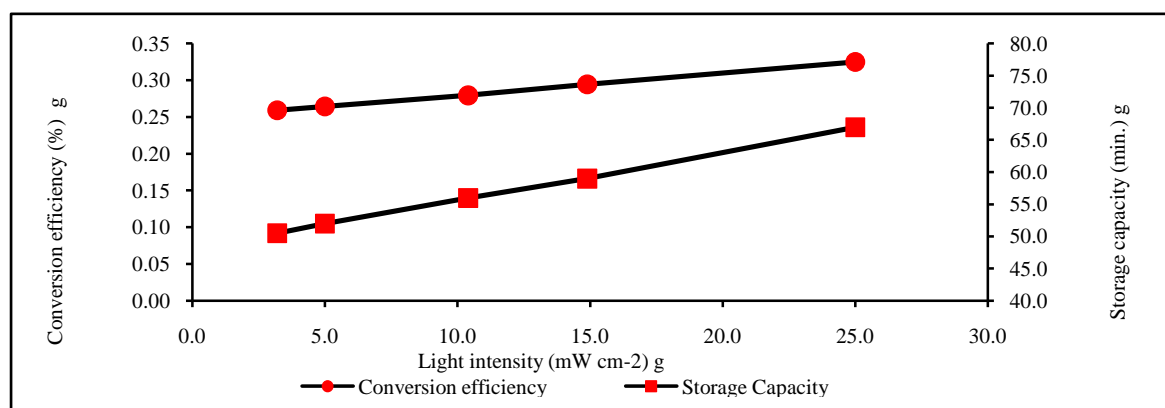


Fig. 3.8: Variation of Conversion efficiency and Storage capacity with Light Intensity

L.Storage Capacity of The Cell

The storage capacity of the photogalvanic cell is observed by applying an external load (necessary to have current at power point) after terminating the illumination as soon as the potential reaches a constant value. The storage capacity is determined in terms of $t_{1/2}$ i.e., the time required in fall of the output (power) to its half at power point in dark. It is observed that the cell can be used in dark for 56.0 minutes for NaLS-Mannose-Azur-B system. Where as in Mannose-Azur-B system (without surfactant) it can be used in dark for 21.0 minutes. The results are reported in following table for NaLS-Mannose-Azur-B system and for Mannose-Azur-B system (without surfactant).

Table 12: Storage capacity of the cell

NaLS-Mannose-Azur-B system		Mannose- Azur-B system [without surfactant]	
[NaLS] = 6.00×10^{-4} Light Intensity = 10.4 mW cm^{-2}		[Mannose] = 1.60×10^{-3}	
[Mannose] = 1.68×10^{-3} Temp. = 303K		[Azur-B] = 5.20×10^{-5}	
[Azur-B] = 5.28×10^{-5} pH = 12.48		pH = 12.17	
Time (Min.)	Power (μW)	Time (Min.)	Power (μW)
0.0	29.07	0.0	10.7
5.0	27.6	2.0	10.3
10.0	26.5	4.0	9.5
15.0	25.2	6.0	9.0
20.0	24.3	8.0	8.8
25.0	23.5	10.0	8.3
30.0	22.8	12.0	7.5
35.0	21.8	14.0	7.1
40.0	20.5	16.0	6.8
42.0	19.7	18.0	6.2
44.0	18.6	19.0	5.7
46.0	17.6	20.0	5.4

48.0	16.8	21.0	5.3
50.0	16.2	22.0	5.2
52.0	15.9	24.0	5.0
54.0	15.2	26.0	4.9
55.0	14.8	28.0	4.8
56.0	14.5		
58.0	13.9		
60.0	12.8		
62.0	12.2		

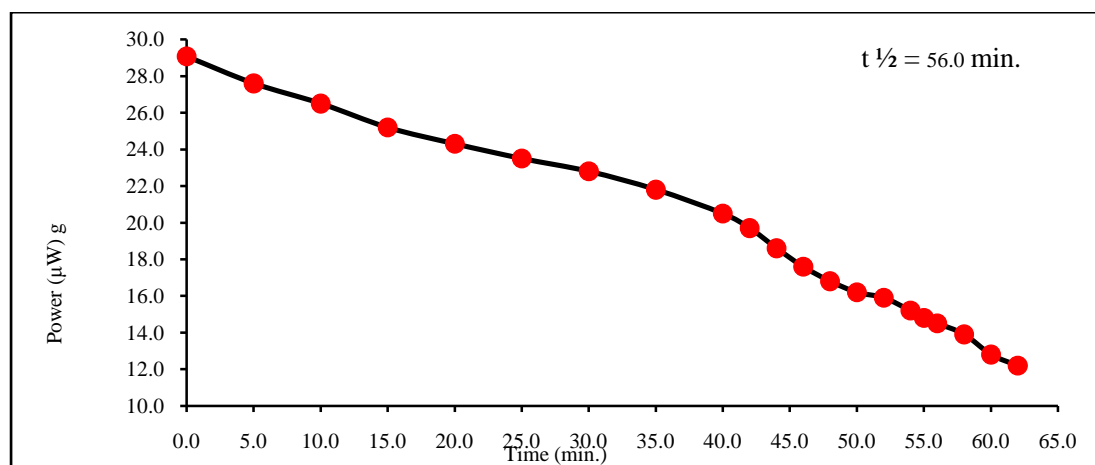


Fig. 3.9 (A): Storage Capacity of the Cell

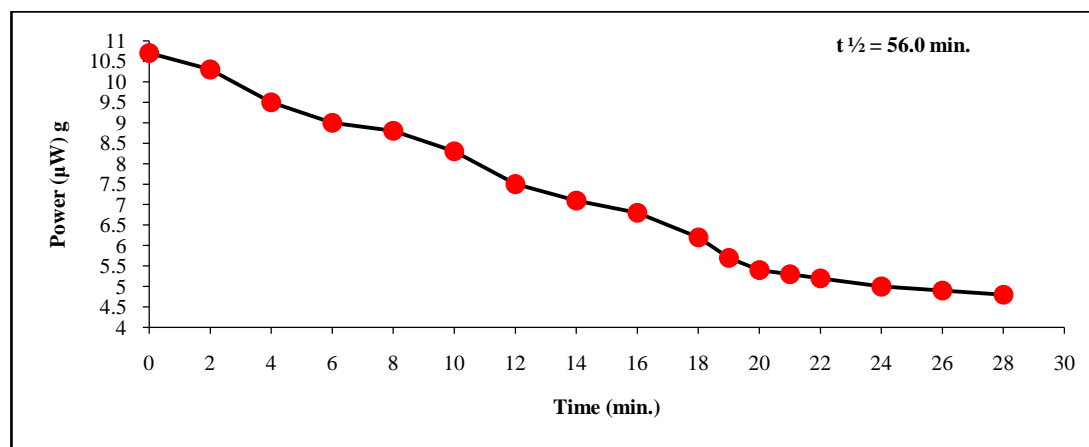


Fig. 3.9: (B) Storage Capacity of the Cell without surfactant

Conversion Efficiency of Cell

The used formula for determine conversion efficiency of the cell is:

$$\text{Conversion Efficiency} = \frac{V_{pp} \times i_{pp}}{10.4 \text{ mW/cm}^2} \times 100\%$$

With the help of current and potential values at Power Point (pp) and the incident power of radiations, the conversion efficiency of the cell is determined as 0.28% in the presence of NaLS-Mannose-Azur-B system where as for Mannose-Azur-B system (without surfactant) the conversion efficiency of this cell is 0.10%.

VI. CONCLUSION

The experimental observation of present work has given an impetus to explore the more suitable selection of surfactant, reductant and photosensitizer to increase the electrical output and storage capacity and lower down the concentration of substrate to reduce the cost of photogalvanic cells. It still has the scope to put up efforts in this direction. The systems to be selected must have surfactants of low cost, high stability along with reductant and photosensitizer. The present study reveals that surfactants have not only increased the conversion efficiency³³⁻³⁵ but also the storage capacity of the photogalvanic cells.

References

1. Wu, N., Plasmonic metal–semiconductor photocatalysts and photoelectrochemical cells: A review. *Nanoscale*, **10**(6), 2679–2696, (2018).
2. Lichtin, N. N., Photogalvanic processes. *Solar Power and Fuels*, 119–142, (1977).
3. Rideal, E. K., and Williams, E. G., XLIII.—The action of light on the ferrous ferric iodine iodide equilibrium. *Journal of the Chemical Society, Transactions*, **127**, 258–269, (1925).
4. Rabinowitch, E., The photogalvanic effect I. The photochemical properties of the thionine-iron system. *The Journal of Chemical Physics*, **8**(7), 551–559, (1940).
5. Rabinowitch, E., The Photogalvanic Effect II. The Photogalvanic Properties of the Thionine-Iron System. *The Journal of Chemical Physics*, **8**(7), 560–566, (1940).
6. Becquerel, A. E. Investigating the effects of chemical radiation of sunlight using electric currents. *CR Acad Sci*, **9**(145), 1, (1839).
7. Malviya, A., and Solanki, P. P. Photogalvanics: A sustainable and promising device for solar energy conversion and storage. *Renewable and Sustainable Energy Reviews*, **59**, 662–691, (2016).
8. Hoffman, M. Z., and Lichtin, N. N., Photochemical determinants of the efficiency of photogalvanic conversion of solar energy. In *Solar energy* (pp. 153-187). Humana Press, (1979).
9. Lu, P., Leung, P., Su, H., Yang, W., and Xu, Q. Materials, performance, and system design for integrated solar flow batteries—A mini review. *Applied Energy*, **282**, (2021). doi.: 10.1016/j.apenergy.2020.116210
10. Koli, P., "Solar energy conversion and storage: Fast Green FCF-Fructose photogalvanic cell." *Applied Energy*, **118**, 231–237, (2014).
11. Koli, P., Sharma, U., and Gangotri, K. M., Solar energy conversion and storage: Rhodamine B-Fructose photogalvanic cell. *Renewable Energy*, **37**(1), 250–258, (2012).
12. Yadav, S., and Lal, C., Optimization of performance characteristics of a mixed dye based photogalvanic cell for efficient solar energy conversion and storage. *Energy Conversion and Management*, **66**, 271–276, (2013).
13. Pokhrel, S., and Nagaraja, K. S., Photogalvanic behaviour of [Cr₂O₂S₂ (1-Pipdte) 2 (H₂O)₂] in aqueous DMF. *Solar Energy Materials and Solar Cells*, **93**(2), 244–248, (2009).
14. Groenen, E. J. J., De Groot, M. S., De Ruiter, R., and De Wit, N., Triton X-100 micelles in the ferrous/thionine photogalvanic cell. *The Journal of Physical Chemistry*, **88**(7), 1449–1454, (1984).
15. Mukhopadhyay, M., and Bhowmik, B. B., Kinetics of photoinduced electron transfer in a photoelectrochemical cell consisting of thiazine dyes and Triton X-100 surfactant. *Journal of Photochemistry and Photobiology A: Chemistry*, **69**(2), 223–227, (1992).
16. Chou, C. S., Chou, F. C., and Kang, J. Y., Preparation of ZnO-coated TiO₂ electrodes using dip coating and their applications in dye-sensitized solar cells. *Powder Technology*, **215**, 38–45, (2012).
17. Kokal, R. K., Bhattacharya, S., Cardoso, L. S., Miranda, P. B., Soma, V. R., Chetti, P., et al., Low cost 'green' dye sensitized solar cells based on New Fuchsin dye with aqueous electrolyte and platinum-free counter electrodes. *Solar Energy*, **188**, 913–923, (2019).
18. Chebrolu, V. T., and Kim, H. J., Recent progress in quantum dot sensitized solar cells: an inclusive review of photoanode, sensitizer, electrolyte, and the counter electrode. *Journal of Materials Chemistry C*, **7**(17), 4911–4933, (2019).
19. Sharma, U., Koli, P., and Gangotri, K. M., Brilliant Cresyl Blue–Fructose for enhancement of solar energy conversion and storage capacity of photogalvanic solar cells. *Fuel*, **90**(11), 3336–3342, (2011).
20. Liu, D., and Kamat, P. V., Electrochemically active nanocrystalline SnO₂ films: surface modification with thiazine and oxazine dye aggregates. *Journal of the Electrochemical Society*, **142**(3), 835–839, (1995).
21. Moreira, L. M., Lyon, J. P., Romani, A. P., Severino, D., Rodrigues, M. R., and de Oliveira, H. P., Phenothiazinium dyes as photosensitizers (PS) in photodynamic therapy (PDT): spectroscopic properties and photochemical mechanisms. *Advanced Aspects of Spectroscopy*, **14**, 393–422, (2012).

22. Koli, P., Dayma, Y., Pareek, R. K., Kumar, R., and Jonwal, M., Simplified photogalvanic cell design with promise for the enhanced solar electricity generation and storage. *Energy Storage*, **4**(1), 1–15, (2022). doi.: 10.1002/est2.287
23. Koli, P., and Sharma, U., Energy conversion in electrolyte under artificial light: Fast Green FCF-Fructose-surfactant-small Pt electrode photogalvanic cell. *Applied Solar Energy*, **52**(2), 76–83, (2016).
24. Koli, P., Pareek, R. K., Dayma, Y., and Jonwal, M., Formic Acid reductant-Sodium Lauryl Sulphate Surfactant enhanced photogalvanic effect of Indigo Carmine dye sensitizer for simultaneous solar energy conversion and storage. *Energy Reports*, **7**, 3628–3638, (2021).
25. Pan, R. L., Bhardwaj, R., and Gross, E. L., Photochemical Energy Conversion by a Thiazine Photosynthetic-Photoelectrochemical Cell. *Journal of Chemical Technology and Biotechnology. Chemical Technology*, **33**(1), 39–48, (1983).
26. Gangotri, K. M., and Regar, O. P., Use of azine dye as a photosensitizer in solar cells: different reductants—safranin systems. *International Journal of Energy Research*, **21** (14), 1345–1350, (1997).
27. Mall, C., Tiwari, S., and Solanki, P. P., Comparison of dye (oxazine and thiazine) materials as a photosensitizer for use in photogalvanic cells based on molecular interaction with sodium dodecyl sulphate by spectral study. *Journal of Saudi Chemical Society*, **23**(1), 83-91, (2019).
28. Suriani, A. B., Nurhafizah, M. D., Mohamed, A., Mamat, M. H., Malek, M. F., Ahmad, M. K., et al., Enhanced photovoltaic performance using reduced graphene oxide assisted by triple-tail surfactant as an efficient and low-cost counter electrode for dye-sensitized solar cells. *Optik*, **139**, 291–298, (2017).
29. Genwa, K. R., and Kumar, A. Dye Sensitized Photogalvanic Solar Cells: Studies in a Methyl Green-NaLS System in View of Energy Conversion. *Energy Sources, Part A: Recovery, Utilization, and Environmental Effects*, **34**(14), 1261–1270, (2012).
30. W.D.K. Clark and J.A. Eckert, Photogalvanic cells. *Solar Energy*, **17**, 147–150, (1975).
31. P.D. Wildest and N.N. Lichtin, *Journal of Physical Chemistry*, **52**, 981, (1978).
32. M. Wyart Remy, A. Kirsch De M. Mesmaeker and J Naslecki, *Nouv. J. Chem.*, **3**, 303, (1979).
33. Koli, P., Solar energy conversion and storage using naphthol green B dye photosensitizer in photogalvanic cells. *Applied Solar Energy*, **50**(2), 67–73, (2014).
34. Koli, P., Photogalvanic cells: Comparative study of various synthetic dyes and natural photo sensitizers present in spinach extract. *RSC Advances*, **4**(86), 46194–46202, (2014).
35. Koli, P., Study of enhanced photogalvanic effect of naphthol green B in natural sunlight. *Journal of Power Sources*, **285**, 310–317, (2015).